Journal of Hydrology: Regional Studies 37 (2021) 100896

Contents lists available at ScienceDirect

Journal of Hydrology: Regional Studies

journal homepage: www.elsevier.com/locate/ejrh

Effects of climate change on terrestrial water storage and basin discharge in the lancang River Basin

Sadia Bibi [a,b,c], Qinghai Song [a,b,c,*], Yiping Zhang [a,b,c], Yuntong Liu [a,b,c], Muhammad Aqeel Kamran [e], Liqing Sha [a,b,c], Wenjun Zhou [a,b,c], Shusen Wang [d], Palingamoorthy Gnanamoorthy [a,b,c]

[a] CAS Key Laboratory of Tropical Forest Ecology, Xishuangbanna Tropical Botanical Garden, Chinese Academy of Sciences, Menglun, 666303, China
[b] Center for Plant Ecology, Core Botanical Gardens, Chinese Academy of Sciences, Xishuangbanna, 666303, China
[c] Global Change Research Group, Xishuangbanna Tropical Botanical Garden, Chinese Academy of Sciences, Menglun, 666303, China
[d] Canada Centre for Remote Sensing, Natural Resources Canada, Ottawa, ON, K1A 0E4, Canada
[e] College of Environmental and Resource Sciences, Zhejiang University, China

ARTICLE INFO

Keywords:
Climate change
TWS
River discharge hydrology
Lancang River Basin

ABSTRACT

Study Region: Lancang River Basin (upper reaches of the Mekong River basin within China).
Study Focus: Complex terranes and diverse climates are a bottleneck for understanding the hydrology of rivers originating from the Tibetan Plateau. This study deals with the impact of climate change on water storage in the Lancang River Basin, which is governed by the South Asian monsoon system. We evaluated the spatiotemporal distribution of multi-source precipitation, evapotranspiration, and terrestrial water storage (TWS) to understand the hydrological system in the region. We provide evidence of climate change impacts on TWS and basin discharge over an upstream region of the transboundary river system.
New Hydrological Insights for the Region: The Five Gravity Recovery and Climate Experiment (GRACE) products and Global Land Data Assimilation System (GLDAS) TWS display analogous seasonal distribution, even though the amounts differ between them. The GRACE and GLDAS TWS exhibited a significant negative trend in the basin from 2002 to 2016. However, the Center for Space Research (CSR-M) at the University of Texas and the Jet Propulsion Laboratory (JPL-M) mascon solutions concede more severe and much wider TWS reduction than the three spherical harmonic (SH) solutions. In addition, a downward trend was observed for basin discharge over 15 years as a response to climate change (decreased precipitation and increased evapotranspiration). Furthermore, we identified a 2-month time lag between precipitation and TWS, which could be a response to climatic factors along with aquifer properties in a karst dominated region.

1. Introduction

The Tibetan Plateau, known as “Asia’s freshwater tower”, is a source region for East and Southeast Asian rivers that serve nearly

* Corresponding author at: CAS Key Laboratory of Tropical Forest Ecology, Xishuangbanna Tropical Botanical Garden, Chinese Academy of Sciences, Menglun, 666303, China.
E-mail address: sqh@xtbg.ac.cn (Q. Song).

https://doi.org/10.1016/j.ejrh.2021.100896
Received 14 April 2021; Received in revised form 12 August 2021; Accepted 16 August 2021
Available online 4 September 2021

half of the world population. The region has shown considerable sensitivity to the impacts of climate change and human intervention, which affect the headwaters of the rivers that originate therein (Ferreira et al., 2020). Therefore, water resource measurements are crucial for understanding the hydrological cycle and water resource management in this region. Observation of climatic variables is a practical approach, as changes in climate variables directly affect the hydrosphere, especially in transboundary rivers where the food, economy, and ecosystem health mainly rely on hydrological and climatic conditions (Liu et al., 2014). The Lancang River originates

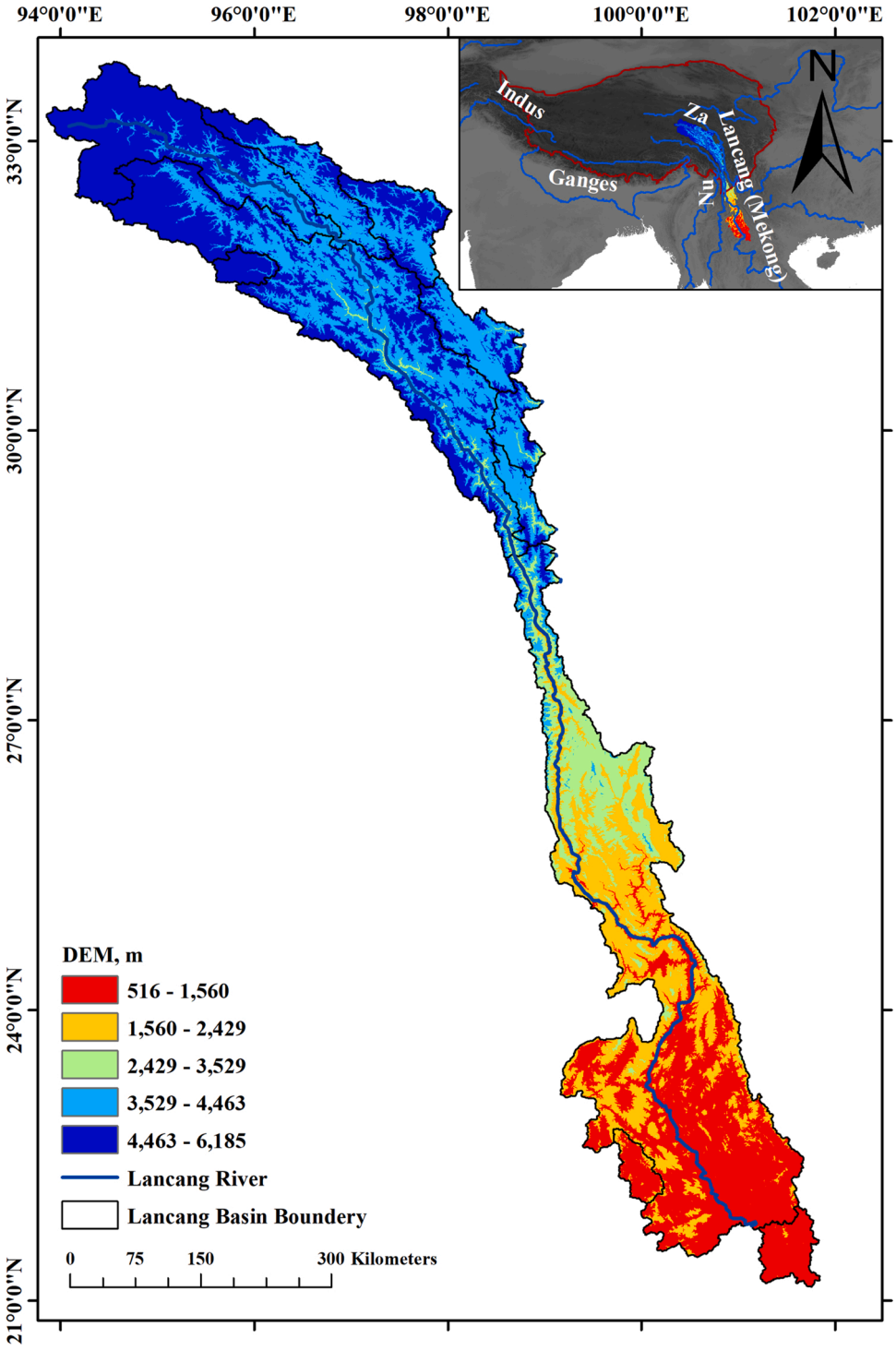

Fig. 1. Digital Elevation Model (DEM) of Lancang River basin.

from the Tibetan Plateau, and with a total area of 795,000 km^2, it is the 12th longest river in the world, feeding more than 60 million people in China, Cambodia, Thailand, Vietnam, Laos, and Myanmar (Jing et al., 2020). The Asian monsoon system, especially the East Asian monsoon and Indian Ocean monsoon systems, are greatly affected by variability in climatic conditions (Wang et al., 2005). Previous studies have recorded a substantial decrease in precipitation over the past several decades in this region (see, e.g., Hasson et al., 2016).

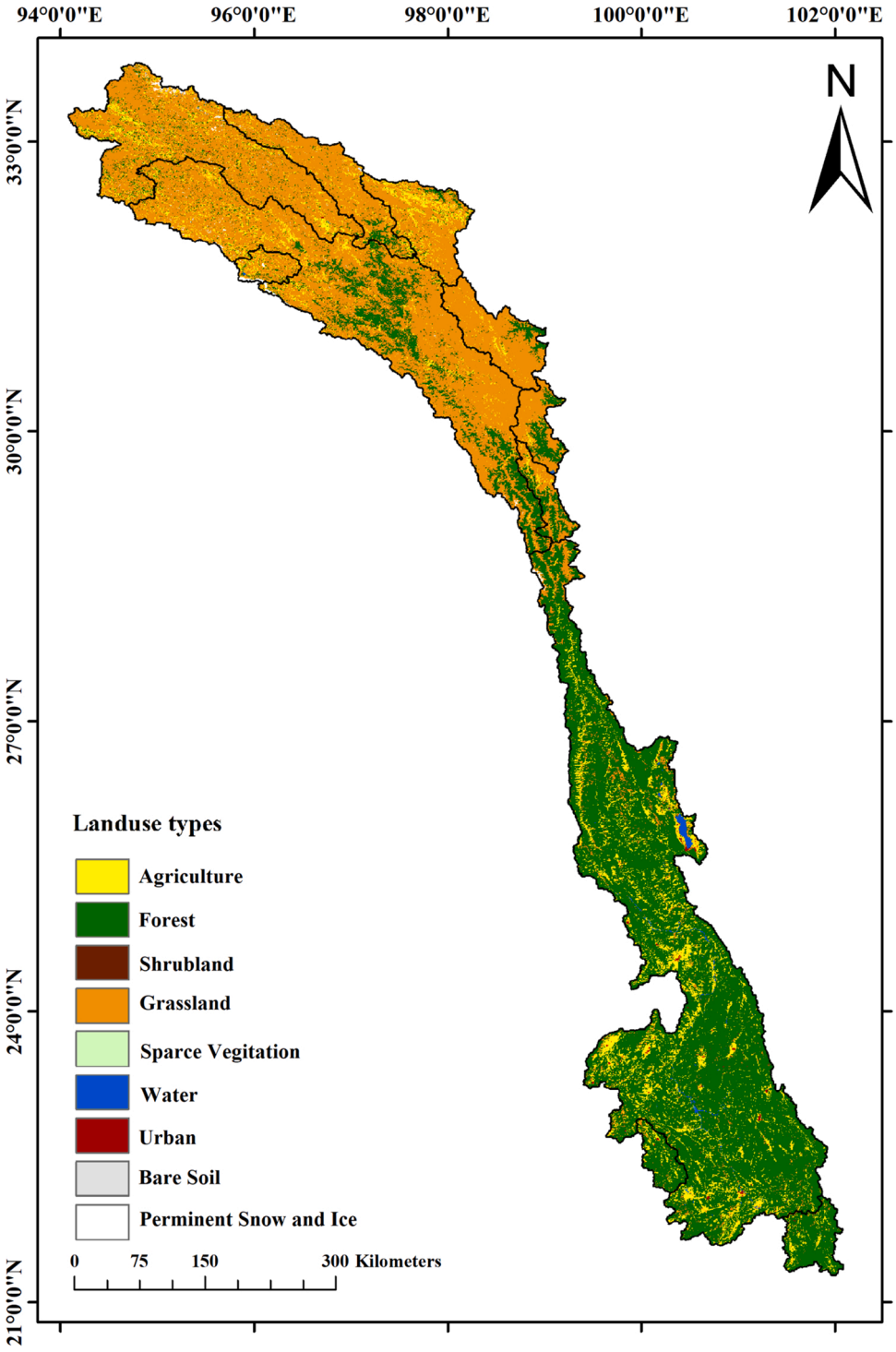

Fig. 2. ESA (2015) landuse map of Lancang River basin.

Global warming accelerates the hydrological cycle process, intensifying the variations in river discharge, regional evapotranspiration, and precipitation. Hence, rising temperatures in the headwaters of the Lancang River add further stress and alter the stream flows and their seasonality, which has affected food production and ecosystem services in the basin (Pokhrel, 2018). The most significant increase in temperature has been recorded during the winter months (Pokhrel, 2018). Water level measurements in the upstream region of the Lancang River before and after dam construction demonstrate similar patterns, suggesting that temperature variation is the primary driver of variation in water level in the headwater region (Li and He, 2008).

Likewise, terrestrial water storage variations (snow, surface water, vegetation water, groundwater, and soil water) provide critical information for evaluating water resource deficit at a regional scale (Andrew et al., 2017; Xie et al., 2016; Ferreira et al., 2020). However, large-scale monitoring of terrestrial water storage (TWS) variations is challenging, as there are limited ground-based monitoring networks and direct means of measurements (Jing et al., 2019). To unravel the coupled energy, water, and carbon fluxes between the atmosphere and land surface, land surface models (LSMs) have been developed, providing direct and indirect measurements in the context of ecological dynamics and human forcing. LSMs are perhaps the most sophisticated tools to estimate individual components of TWS, especially root zone soil moisture and groundwater assessment, which are far beyond the capacity of typical microwave and optical sensor-based satellites (JPL, 2018). However, to monitor the temporal gravity field changes on Earth, the Gravity Recovery and Climate Experiment (GRACE) satellite launched in 2002 provides ease in obtaining unique data (TWS) that reflects mass transport and redistribution above and beneath the surface of Earth (Landerer and Swenson, 2012b; Seyoum and Milewski, 2017; Wahr et al., 2004). GRACE provides comprehensive information on vertically integrated water storage changes by recording gravity field changes on Earth (Jing et al., 2019; Landerer and Swenson, 2012b;Landerer and Swenson, 2012b) and offers more direct ways of TWS estimations than LSMs (Jing et al., 2019). GRACE provides TWS data in two versions: mascon (M) and spherical harmonic (SH) solutions calculated by mass concentration blocks (mascons) and standard spherical harmonic approaches (Scanlon et al., 2016b; Landerer and Swenson, 2012b). These GRACE products have been widely used to investigate TWS variations in numerous studies, including transboundary river basins (e.g., Lancang-Mekong River Basin) across the globe (Long et al., 2013; Jing et al., 2020; Bibi et al., 2019). In this study, we used GRACE products, including SH solutions from the Jet Propulsion Laboratory (JPL), GeoForschungsZentrum (GFZ), and the Center for Space Research at the University of Texas, Austin (CSR) and M solutions from the JPL (JPL-M) and CSR (CSR-M) to calculate river discharge in the Lancang River Basin using the water balance method. We calculated river discharge using the GLDAS L and surface models, GLEAM and TWS, and precipitation data from space observations.

This study provides a comprehensive insight into the spatiotemporal distribution of water balance components and TWS in the Lancang River Basin and how they affect river discharge. We discuss the relative importance of climatic factors and their influence on TWS variations. The primary objectives of this study were 1) to describe spatiotemporal variations in precipitation, evapotranspiration, temperature, and TWS trends derived from different solutions using the basin-average approach; 2) to estimate the total basin discharge in the study region based on the water balance method, and 3) to estimate the time lag between precipitation and TWS and explore the factors that may impact the time lag. These findings could be helpful for water resource management and utilisation in transboundary river basins.

2. Study area and data resources

2.1. Study area

The Lancang-Mekong River, which originates from the southern Tibetan Plateau, is the 7th largest river in Asia. The Lancang River Basin (Fig. 1) (21 °N–34 °N; 94 °E–102 °E) is 2354 km long with a drainage area of approximately 165,000 km^2 and an elevation range from approximately 486 to 6500 m above sea level (Tang, 2010). The Lancang River Basin covers different climatic zones with diverse geographic conditions, resulting in a striking difference in water resources and heat distribution in this region. The annual mean precipitation increases from north to south and ranges from 752 to 1025 mm. Similarly, temperature increases from north to south and ranges between 12.3 and 14.3 °C.

The Lancang River Basin is located in the tropical monsoon region of Southeast Asia. The seasonal cycle is divided into wet (May to October), with a peak in August and a dry season (November to April). Most of the area is occupied by forests in the southern part of the basin, while grassland is the main land-use type in the northern high-altitude region (Fig. 2).

2.2. GRACE-derived TWS

2.2.1. Spherical harmonics solutions (RL06)

The GRACE satellites provide monthly global total water storage anomalies by measuring gravity field changes on Earth. The SH solution has been the standard for the first decade of GRACE observations (Landerer and Swenson, 2012b; Vishwakarma et al., 2018). The official GRACE Science Data System has continuously released monthly GRACE solutions from three processing centers: (1) Center for Space Research, University of Texas (CSR), (2) Jet Propulsion Laboratory (JPL), and (3) GeoForschungsZentrum (GFZ) available at https://grace.jpl.nasa.gov/data/get-data/monthly-mass-grids-land/. The time series of the TWS anomalies from the three processing centers were averaged to reduce the uncertainties in the TWS estimate. Different GRACE solutions use different strategies and parameter choices (Sakumura et al., 2014).

2.2.2. The global mascon

GRACE mascon solutions are produced using mass concentration blocks (mascons) (Scanlon et al., 2016b). It is much easier to

implement geophysical constraints for mascon solutions, and this approach is much more rigorous than the spherical harmonics of empirical post-processing filtering (Landerer and Watkins, 2016). CSR-M and JPL-M solutions are available at https://grace.jpl.nasa.gov/data/get-data/monthly-mass-grids-land/. The latest release (V3) is RL06 gravity field solutions with a spatial resolution of 0.25 ° × 0.25 °, but the native resolution is 1 ° × 1 ° (Save et al., 2016).

2.3. Evapotranspiration data

The Global Land and Data Assimilation System (GLDAS) uses several offline land-surface models to assimilate enormous observational data at high resolutions globally. The GLDAS_Noah2.1 dataset with 0.25 ° × 0.25 ° resolution (Rodell, 2004) is available at https://disc.gsfc.nasa.gov/. We used GLDAS_Noah 2.1 evapotranspiration data (kg m^{-2} s^{-1}) in the current study. GLDAS-Noah-2.7.1 land hydrology model data (https://grace.jpl.nasa.gov/data/get-data/land-water-content/) called land water content has been used for monthly TWS change estimation in the basin. Furthermore, we used the Global Land Evapotranspiration model from Amsterdam (GLEAM 3.3a). The GLEAM model estimates daily terrestrial evapotranspiration from satellite data at a 0.25 ° spatial resolution and is available at https://www.gleamproject.org/data.

2.4. Precipitation and temperature data

In the present study, we obtained temperature and precipitation data sets (2001–2015) from the National Meteorological Information Centre of the Meteorological Administration of China (CMA). These datasets have a horizontal resolution of 0.5 ° × 0.5 ° and are available at the CMA data-sharing service system (http://cdc.cma.gov.cn/home.do).

The Tropical Rainfall Measuring Mission (TRMM) is a multi-satellite precipitation product from NASA, available at http://trmm.gsfc.nasa.gov/data_dir/data.html. TRMM merges data from various satellite sensors and rainfall-gauge observations from the Global Precipitation Climatology Centre. Therefore, the rainfall data from TRMM were considered to be of good quality for the subsequent analysis.

3. Methods

3.1. Precipitation and evapotranspiration anomalies

Terrestrial water storage changes from GRACE solutions are available as anomalies and computed by averaging from January 2004 to December 2009 (Ramillien et al., 2006). Therefore, we used the same approach to calculate the precipitation and evapotranspiration anomalies for the Lancang River Basin. Anomalies were calculated relative to the mean values of precipitation and evapotranspiration averaging from January 2004 to December 2009.

3.2. Basin discharge calculation

The traditional water balance approach, Eq. (1), is the most widely used method and is an integral part of any conceptual model based on the principle of mass conservation. The mass balance equation using GRACE data can be arranged as follows:

$$\frac{d(TWS)}{dt} = P - ET - R \tag{1}$$

In previous studies, the water balance method has been used to calculate monthly basin discharge (Gao et al., 2010; Lv et al., 2017). We applied the same approach to calculate the basin discharge for the Lancang River Basin in our study by rearranging Eq. (1); recharge can then be calculated as shown in Eq. (2):

$$R = P - ET - \frac{d(TWS)}{dt} \tag{2}$$

Where R is the monthly total basin discharge, ET is evapotranspiration, P is precipitation, and $\frac{d(TWS)}{dt}$ is the TWS anomaly from the five GRACE solutions. The submarine discharge, potential interbasin leakage, and water diversion were not considered in Eq. (2), as suggested by Ferreira et al. (2013): The average ET was calculated from GLDAS (averaged from Noah, VIC, and CLM), and precipitation was obtained from TRMM. In the monthly time series of GRACE TWS data, a few months were missing during the study period due to satellite battery management issues. These missing months were filled using the spline interpolation method.

3.3. Trend analysis

3.3.1. Linear regression

To scrutinise the linear trend of the variables, a simple linear regression equation can be written as:

$$yx = a + bx \tag{3}$$

Where 'yx' symbolises the parameters at time 'x'; the intercept 'a' and slope 'b' are regression coefficients obtained by the least square

method. Student's *t*-test was performed to test the statistical significance of the trend.

3.3.2. Mann-Kendall test

The Mann-Kendall test has wide-ranging applications as a statistical test in climatological and hydrological trend analysis (Mavromatis, 2011) . Mann-Kendall trend analysis has two main advantages: (1) it is a non-parametric test that does not require data to be

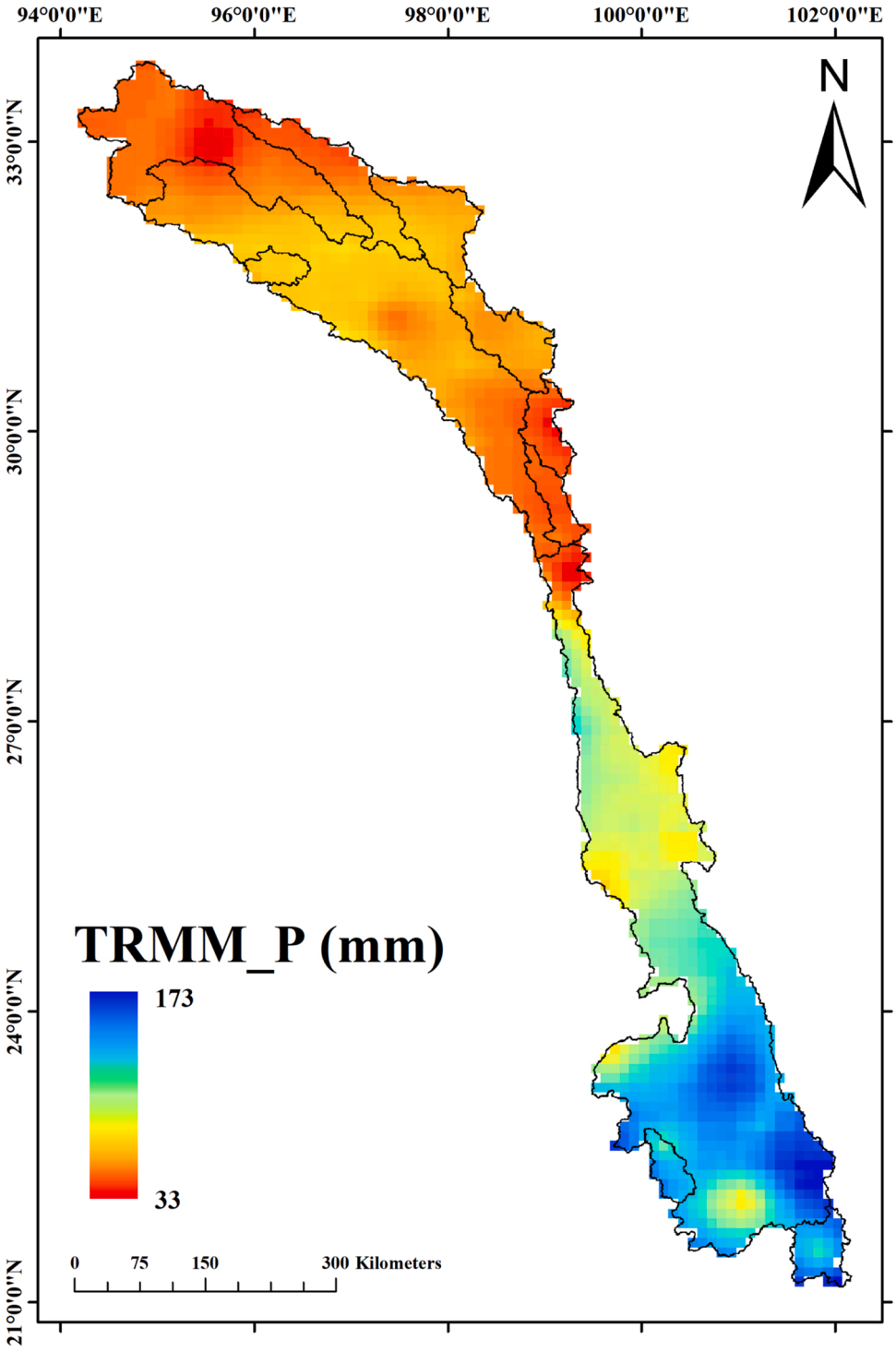

Fig. 3. Spatial variation of TRMM precipitation (mm/month).

normally distributed, and (2) it is less sensitive to unexpected interruptions in nonhomogeneous time series (Tabari, 2011). For uncertainty against time, (Mann, 1945) developed a non-parametric test for precise application of Kendall's test for correlation which is commonly known as the 'Mann-Kendall test' or 'Kendall *t* test' (Kendall, 1975). He proposed the null hypothesis as 'H0′, for a population (X1, X2,. . ., Xn) and 'H1′ as an alternative hypothesis. The Mann-Kendall test statistic under 'H0′ is given as follows:

$$S = \sum_{i=1}^{n-1} \sum_{j=i+1}^{n} sgn(x_j - x_i) \tag{4}$$

Where

$$sgn(\theta) = \begin{cases} +1.....\theta > 0 \\ 0.....\theta = 0 \\ -1.....\theta < 0 \end{cases} \tag{5}$$

For independent and randomly distributed random variables, when $n \geq 8$, the 'S' statistic is approximately normally distributed, with zero mean and variance, as follows:

$$\sigma^2 = \frac{n(n-1)(2n+5)}{18} \tag{6}$$

Consequently, the standardised 'Z' statistics follow a normal standardised distribution:

$$Z = \begin{cases} \dfrac{S-1}{\theta} \; if \; S > 0 \\ 0 \; if \; S = 0 \\ \dfrac{S+1}{\theta} \; if S < 0 \end{cases} \tag{7}$$

The no trend hypothesis is rejected when 'Z' > '$Z\alpha$' (Eq. 7) at a level of significance 'α'. In the present work, we used Mann-Kendall analysis for spatial interpolation of the TWS time series as a few months were missing from the GRACE record during the study period.

4. Results

4.1. Precipitation and evapotranspiration trends in Lancang River basin

The Lancang River Basin comprises diverse topography. Fig. 3 shows considerable variation in the spatial distribution of precipitation amount, which was low at high elevation and increased with decreasing elevation, ranging between 33–173 mm. Annual precipitation displayed a decreasing trend, and the rate of decrease was -5.03 mm/year (Fig. 4). Evapotranspiration is a very important climate variable; hence, careful data selection was crucial for further analysis. Accordingly, we used average evapotranspiration data from the GLDAS (Noah, VIC, and CLM) models and GLEAM to remove the uncertainty in the results (Andam-Akorful et al., 2015). Both GLDAS and GLEAM evapotranspiration had an increasing trend of 4 and 4.1 mm/year, respectively, from 2002 to 2020 (Fig. 5(b)).

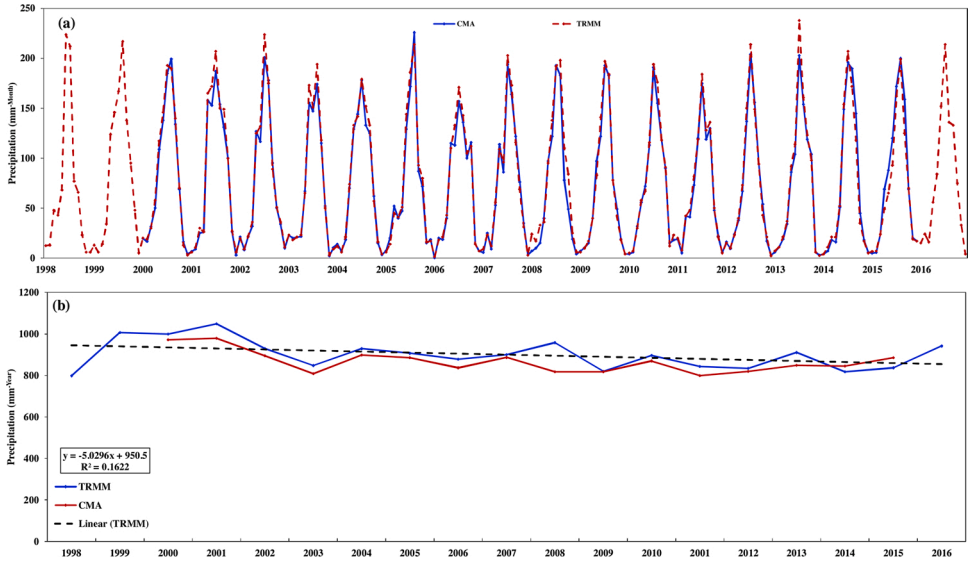

Fig. 4. Precipitation from CMA gridded data and TRMM (CMA 2000-2015), (TRMM 1998-2016) mean monthly (a) and yearly (b) precipitation.

Fig. 6(a) illustrates the spatial patterns of evapotranspiration distribution from the GLDAS (Noah, VIC, and CLM) and GLEAM models. The amount of evapotranspiration upstream of the Lancang River Basin was observed to be much lower than that of the downstream region and ranged between 21 and 105 mm/month. The spatial M-K trend analysis of evapotranspiration from the Noah and VIC models presented an increasing trend (Fig. 6(b)) in downstream and most of the upstream regions of the basin, whereas the CLM model presented a varying trend of an increase, decrease (in red), and no trend (in green) in the basin. GLEAM also exhibited increasing trends in evapotranspiration both upstream and downstream of the basin. Fig. 7 shows the scatter matrix map between Noah, VIC, and CLM evapotranspiration of the Lancang River Basin; Noah and VIC were found to have a stronger correlation than Noah and VIC with CLM. Therefore, using average evapotranspiration from the three GLDAS models and GLEAM in further analysis minimises the uncertainty in evapotranspiration estimates in the basin.

4.2. GRACE TWS trends

4.2.1. Temporal TWS trends from different GRACE solutions and GLDAS

Fig. 8(a–b) illustrates the monthly mean linear distribution of TWS from the five GRACE solutions (2002–2016), GRACE-FO (2018–2020), and GLDAS TWS. Fig. 8(b) shows the linear trends of GRACE solutions and GLDAS-TWS, where the dotted lines represent the linear trends of the five GRACE TWS and GLDAS-TWS. As shown in Fig. 8(b), all five GRACE TWS and GLDAS-TWS show decreasing trends in the Lancang River Basin. CSR-M and JPL-M trends were more significant than SH solutions from CSR, GFZ, and JPL because SH products might experience signal leakage in the region, which deserves further investigation as this was not addressed in the present study. TWS from the five GRACE products exhibited an increasing trend from 2006 to 2008 and then decreased afterwards, agreeing with a previous study (Jin et al., 2020). Generally, all five solutions showed a decreasing trend during the entire study period in the region. The GLDAS TWS trends were in good agreement with GRACE TWS, with a decreasing trend of 4.0 mm/year in the Lancang River Basin.

Table 1 summarises TWS trends derived from the different GRACE solutions. Trend analysis revealed that both SH (CSR, GFZ, and JPL) and CSR-M had a significant decreasing trend in TWS during the study period. JPL showed a decreasing trend of -3.3 mm/year, CSR -3.5 mm/year, GFZ -3.2 mm/year, JPL-M -6.0 mm/year, and CSR-M -5.0 mm/year. However, the JPL-M solution revealed a more severe and much wider TWS reduction in the study region. The GLDAS-TWS showed a decreasing trend of -4.0 mm/year, which was in good agreement with CSR, GFZ, and JPL. The five GRACE products and the GLDAS TWS revealed similar seasonal variability, regardless of the different volumes between them.

4.2.2. Spatial TWS trends from GRACE solutions and GLDAS

Fig. 9 shows the spatial distribution of the GRACE TWS derived from the five solutions. It can be seen that TWS distribution in the Lancang River Basin opposed the elevation gradient, low at high elevation (upstream) and high at low elevation (downstream; Fig. 9 (a)). A substantial loss in TWS in the high elevation (upstream) river source region during the entire period was observed, and the declining trend was consistent for all GRACE solutions [(Fig. 9(b)]. Previous studies have reported that a massive decline in TWS in the Indian monsoon-dominated Tibetan Plateau region is caused by rising temperatures and decreased precipitation in the Himalayas (Yao, 2012; Jing et al., 2020). Additionally, a previous study reported groundwater depletion upstream, which added stress to TWS in the headwater region of the Lancang River (Yi et al., 2016). In downstream water, storage was substantially increased, but this increase could be due to the construction of large reservoirs in lowland areas which appeared to increase water storage downstream (Eyler, 2020). A previous study reported a significant decrease in river flow recorded at the Yungjinghong hydrometric station located

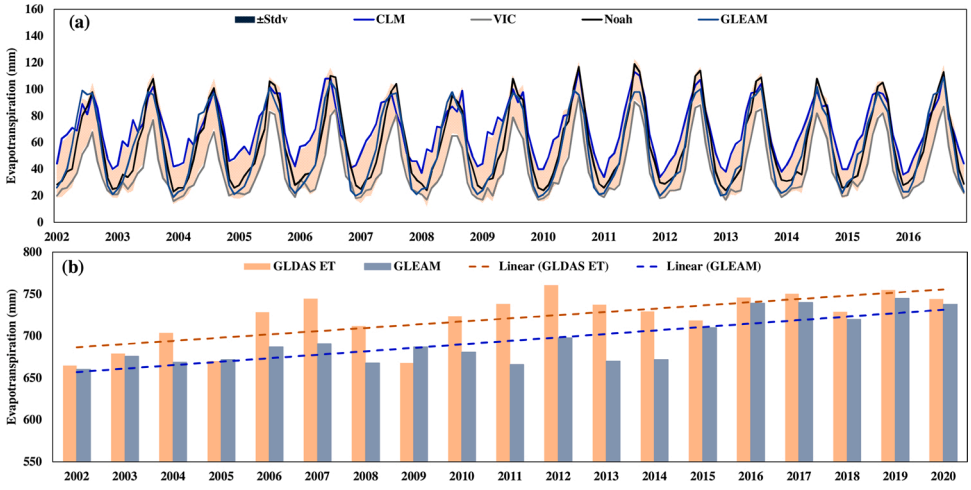

Fig. 5. Monthly average evapotranspiration from GLDAS (Noah, VIC and CLM) and GLEAM (mm/month 2002-2016) (a) and yearly mean (mm/year 2002-2020) (b). The shaded area in (a) is ± Standard deviation.

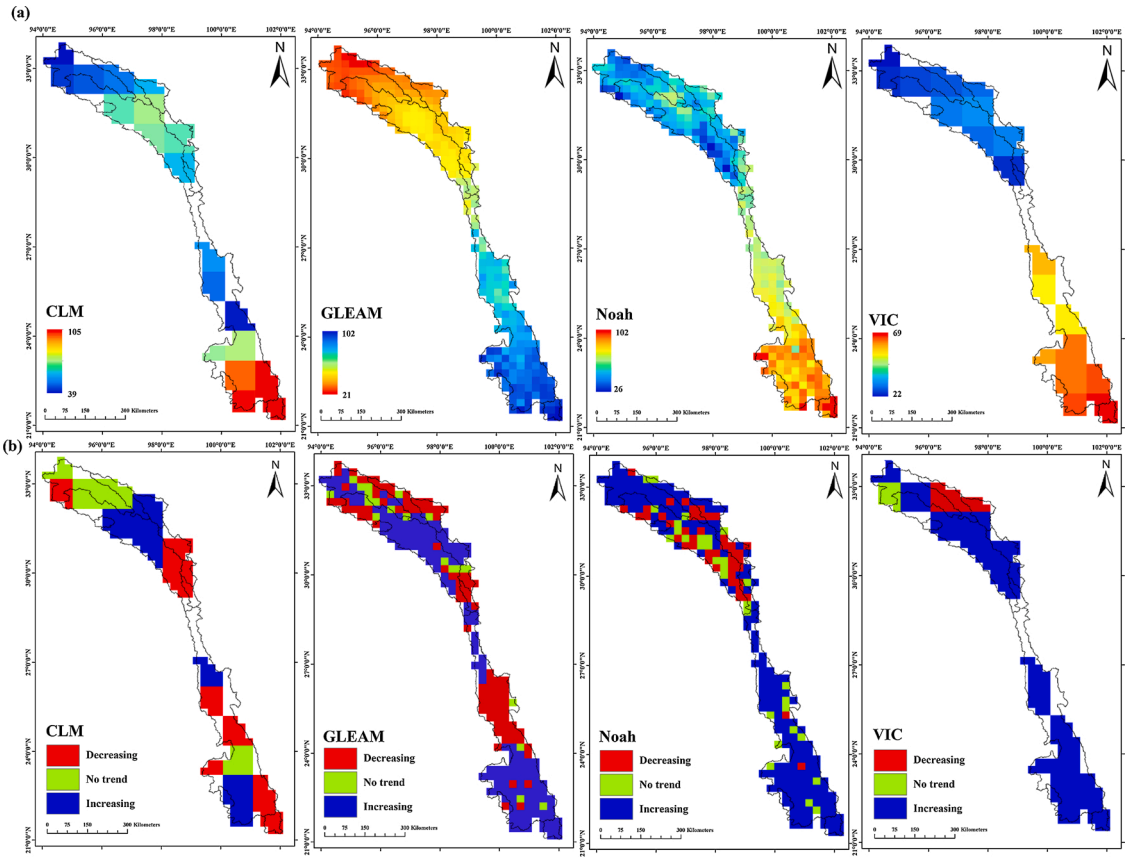

Fig. 6. GLDAS (Noah, VIC, and CLM) and GLEAM evapotranspiration (mm/month) (a) and M-K trend analysis (b) (2002-2016) over Lancang River basin.

downstream of the basin from 1961 to 2015 (Liu et al., 2020).

It is clear from Fig. 9(b) that the spatial distribution of TWS solutions showed some discrepancies; JPL-M exhibited a slightly deviating trend from the other four GRACE solutions. Previous studies have reported that the decreasing and increasing trends of the JPL-M TWS are comparatively larger than those of other CSR-M and SH solutions (Scanlon et al., 2018; Jin et al., 2020). The three processing centers (JPL, GFZ, and CSR) use different mathematical approaches and background models for the GRACE TWS calculation. For instance, JPL-M uses the glacial isostatic adjustment (GIA) correction model, which has not been considered for other GRACE solutions (Purcell et al., 2016). Additionally, JPL and CSR centers use dissimilar data processing techniques for global mascon solutions; JPL-M calculations employ spherical cap mascons (3 ° equal-area), whereas CSR-M uses hexagonal tiles (1 ° equatorial longitudinal distance) (Watkins et al., 2015; Scanlon et al., 2016b; Purcell et al., 2016). The correlation and scatter matrix maps in Fig. 10 indicate that the temporal distribution of the five GRACE solutions is highly consistent; however, CSR-M and JPL-M are more consistent with each other than with the SH solution. In contrast, JPL-M and CSR-M correlated significantly ($r = 0.98$), reaching minimum and maximum values almost simultaneously.

4.3. *Total basin discharge*

Fig. 11 illustrates the temporal trends of the total basin discharge in the Lancang River Basin from 2002 to 2015. The time series of the total basin discharge were calculated as a residual of the water balance (Eq. 2) using precipitation (TRMM and CMA), evapotranspiration (averaged from GLDAS Noah, VIC, and CLM models), and TWS time-series estimates. The total basin discharge calculated from JPL-M and CSR-M using both CMA and TRMM precipitation revealed a continuous decreasing trend in the basin. Basin discharge from CMA precipitation revealed decreasing trends of -56 and -70 mm/year for the JPL-M and CSR-M TWS, respectively. Likewise, the discharge calculated using TRMM was -70 mm/year for JPL-M and -63 mm/year for CSR-M. Similarly, the total basin discharge calculated using GLEAM evapotranspiration for JPL-M and CSR-M using CMA and TRMM precipitation showed an incessant decreasing trend. Basin discharge from CMA precipitation revealed decreasing trends of -56 and -74 mm/year for the JPL-M and CSR-M TWS, respectively. Likewise, the discharge calculated using TRMM was -57 mm/year for CSR-M and -71 mm/year for JPL-M. The basin discharge trend was similar to that of precipitation (Fig. 4) and TWS (Fig. 8). Increased evapotranspiration (Fig. 5) with decreasing precipitation resulted in decreased basin discharge during the study period.

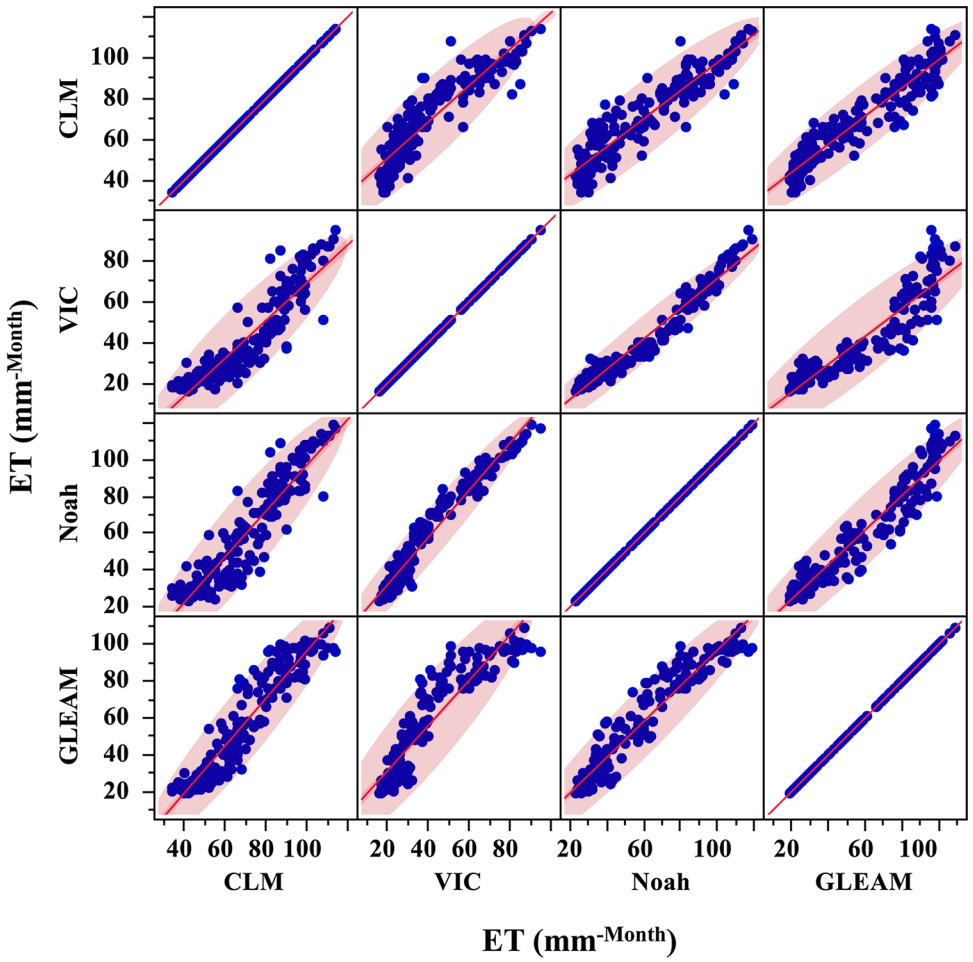

Fig. 7. Scatter matrix between Noah, VIC, CLM, and GLEAM ET over Lancang River basin (red lines are linear fit and the red shaded area is density distributions). (For interpretation of the references to colour in the Figure, the reader is referred to the web version of this article).

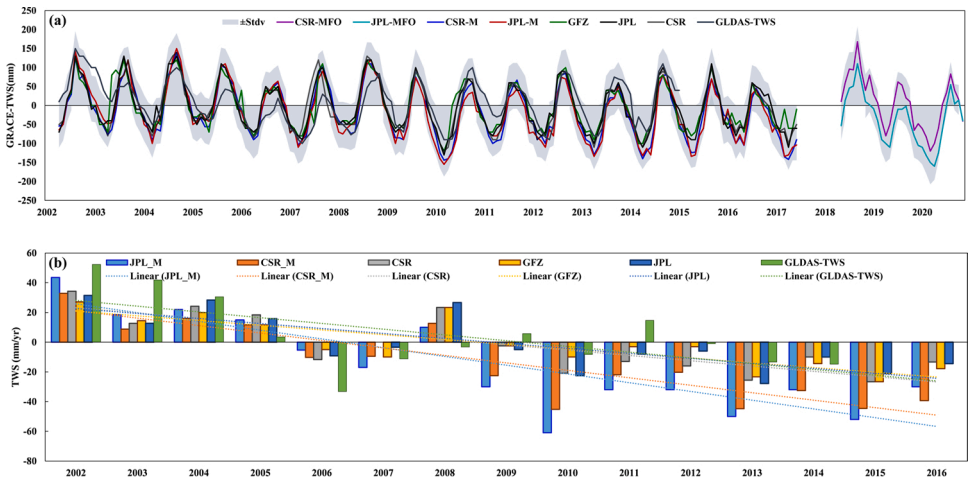

Fig. 8. GRACE (2002-2016) and GRACE-FO (2018-2020) from CSR-M, JPL-M, GFZ, JPL, CSR from SH, and GLDAS-TWS (2002-2014) (a) monthly and (b) yearly mean in Lancang basin.

Table 1
Terrestrial water storage trends from different GRACE solutions and GLDAS in Lancang River Basin.

	Solutions	Trends mm/year	R^2	Standard Deviation
1	JPL	−3.3	0.60	±19
2	GFZ	−3.2	0.70	±17
3	CSR	−4.0	0.66	±20
4	CSR-M	−5.0	0.87	±25
5	JPL-M	−5.9	0.72	±31
6	GLDAS-TWS	−4.0	0.40	±24

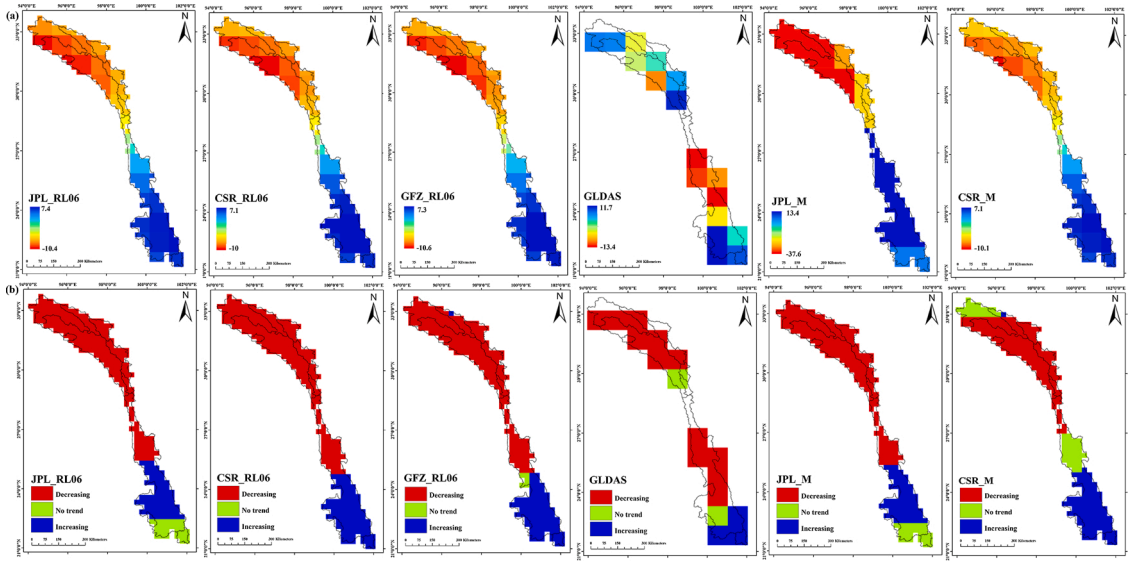

Fig. 9. The spatial distribution of five GRACE-TWS and GLDAS-TWS (a) and M − K trends of GRCAE-TWS and GLDAS-TWS (b) in Lancang basin (2002-2016).

4.4. Warming trends in Lancang River Basin

The mean temperature distribution in the Lancang River Basin, M-K trend analysis, and temporal distribution and seasonality are shown in Fig. 12(a–d). Spatially, the mean temperature was low (-8.3 °C) in the high-altitude mountainous region upstream of the basin and decreased towards the south downstream (23 °C) [Fig. 12(a)]. However, the temperature exhibited a significant increasing trend over the study period in both the upstream and downstream parts of the basin (Fig. 12(b)). It can also be seen in Fig. 12(c) that, temporally, the temperature rose at a rate of 0.05 °C from 2002 to 2015 in the study region. Hence, the spatiotemporal trends of mean temperature depict massive warming in the Lancang River Basin. This increase in warming rate is alarming given that the Lancang River Basin comprises the upper part of the Mekong River Basin, feeding more than 60 million people worldwide, including China and the countries located downstream (Cambodia, Thailand, Vietnam, Laos, and Myanmar) (Jing et al., 2020). Increased warming is responsible for increased evapotranspiration in the study region, which negatively impacts the available water resources in this region.

5. Discussion

The Lancang River is situated in a complex environmental setting with roughly two diverse topographies that gradually transform from grassland-dominated plateaus to tropical rainforest zones in the south. Topographic gradients and diverse climates control the distribution of water resources across basins. The downward trend in precipitation and a higher evapotranspiration rate have significantly contributed to the reduction of TWS and total basin discharge in the Lancang River Basin. Previous studies detected severe drought in southwest China in 2009 and 2010 (Yang, 2012), which agrees well with our results. Fig. 12(c) demonstrates that the highest annual mean temperature was recorded in 2009, while the mean annual precipitation was below average during the same year (Fig. 4(b)). The Lancang River Basin is located in a karst region, where shallow soils have high permeability, leading to water stress during the dry season. (Yang et al., 2019).

The Lancang River Basin is located in a typical South Asian monsoon-dominated region, the most prominent monsoon system globally (Song, 2012). Fig. 13(c) reveals that precipitation has a clear seasonal cycle due to the South Asian monsoon effect. During July and August (wet monsoon season), the basin receives 70–80 % of its annual total precipitation. Climate change in this region not only drives the precipitation cycle but also influences TWS. Under increased warming and decreased precipitation, CSR, JPL, GFZ,

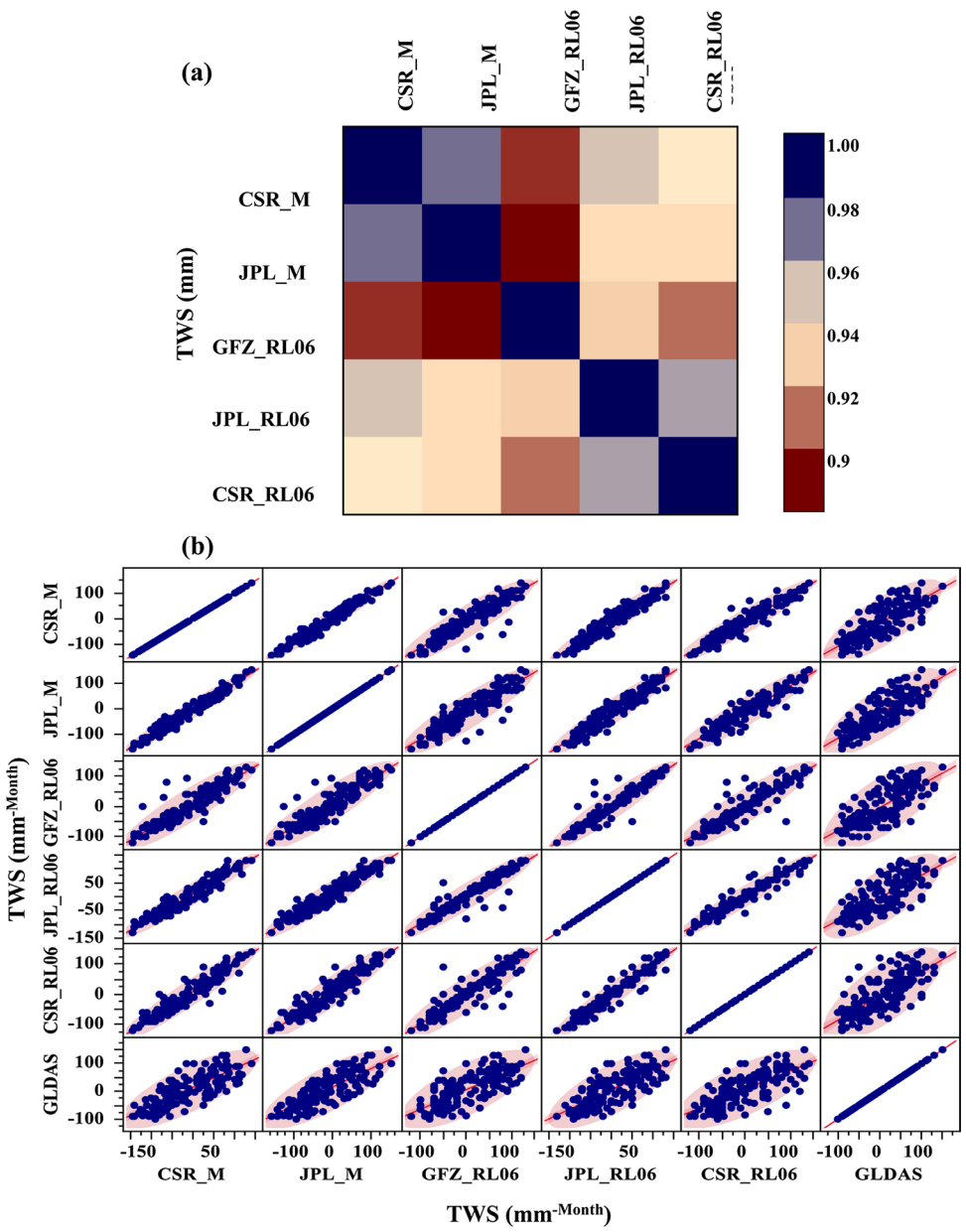

Fig. 10. Correlation map between CSRM,JPLM,GFZ,CSR,and JPLT WS solutions (a)and scatter matrix between GRACE TWS solutions (b) in Lancang River basin (red lines are linear fit and the red shaded area is density distribution). (For interpretation of the references to colour in the Figure, the reader is referred to the web version of this article).

CSR-M, and JPLM from GRACE and GLDAS-TWS showed decreasing trends in TWS during the study period. The impact of climate change on TWS is evident from the 2009–2010 drought, as shown in the TWS anomalies of the five GRACE solutions (Fig. 8(b)), indicating that climatic factors are the main driving forces behind TWS variations in this region. Furthermore, Fig. 8(b) indicates that the CSR-M and JPL-M solutions are more sensitive to climate variations than the three spherical harmonic solutions, as the 2009–2010 drought is more evident in both mascon solutions. Drought does not appear in GLDAS-TWS because the GLDAS land water content does not include groundwater and surface water, i.e., lakes and rivers, as separate water components in its calculation. In agreement with our results, downward trends in precipitation and increased temperature has been reported as the main contributors to TWS variations in the river source region (Tibetan Plateau) (Yao, 2012; Jing et al., 2020; Yang et al., 2019; Qiao et al., 2015; Bibi et al., 2018). Moreover, Yi et al. (2016) reported that groundwater depletion in the upstream region of the Lancang River Basin in the Tibetan Plateau added more stress to TWS, and it is evident in Fig. 9(b) that all the GRACE solutions and GLDAS TWS showed a significant decreasing trend upstream of the basin during the study period.

The basin discharge for the Lancang River was calculated as a residual from TWS, precipitation, and evapotranspiration using the

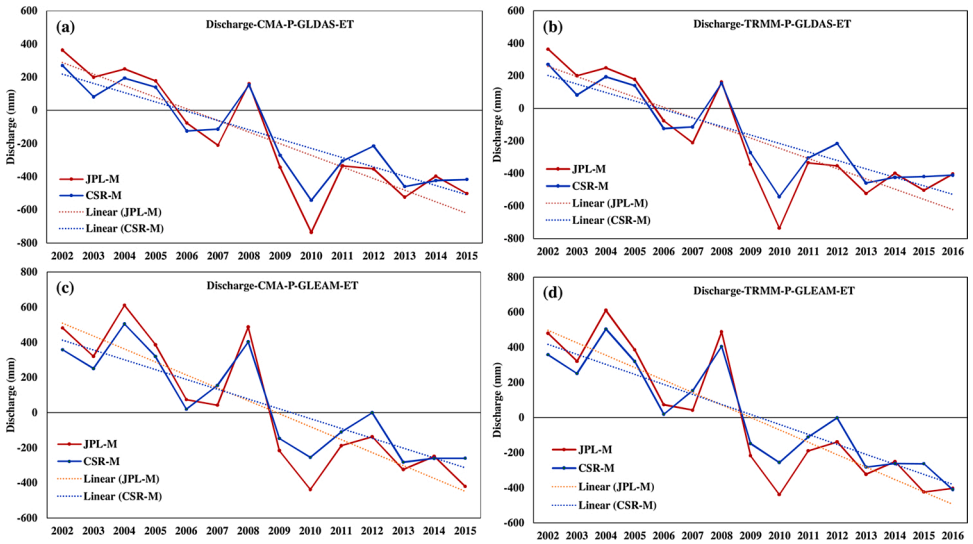

Fig. 11. Total basin discharge from JPL-M and CSR-M by GLDAS ET and CMA and TRMM precipitation (a-b) and total basin discharge from JPL-M and CSR-M by GLEAM ET and CMA and TRMM precipitation (c-d).

basin average approach. Discharge showed a significant decreasing trend in the basin, using both CMA and TRMM precipitation, as opposed to the two GRACE mascon solutions (Fig. 11(a–b)). Given that the Lancang is a transboundary river, the observation data is under government control, and access to observations requires multi-party government permission and cooperation. To support our findings, we compared our results with the river flow recorded at the Yungjinghong hydrometric station located on the Lancang River, which showed a significant decreasing trend in river flow from 1961 to 2015 (Liu et al., 2020).

Fig. 13(a–b) shows a time lag of 2 months between TWS anomalies derived from the JPL-M and CSR-M and precipitation. The highest precipitation was recorded in July, while the highest TWS was recorded in September. In a hydrosphere, when precipitation is converted to TWS during the water distribution process, there is the possibility of a theoretical delayed response between TWS and precipitation (Xu et al., 2018). Assessing the precise time lag between precipitation and TWS as lag variations is decisive in understanding the interactions between climate variables and the hydrosphere. A study conducted by Syed et al. (2008) demonstrated that GLDAS-TWS strongly correlates with precipitation in low-latitude regions. In the Tibetan Plateau, a 2-month lag has been identified between GRACE-TWS and precipitation in the three river source regions (Xu et al., 2018). Thus, precipitation is a key driver of the water budget and has immense control over the hydrological cycle and water balance in this region. Furthermore, numerous studies have been conducted to reveal and understand the phenomenon behind the time lag between TWS and precipitation. There is a delay in the TWS response when water enters the system as precipitation and distributes into the surface and subsurface water; empirically, lag can be defined as the total precipitation in hydrological balance (Thompson et al., 2011). In the present study, GRACE-TWS anomalies from CSR and JPL mascon solutions were highly correlated with precipitation over a 2-month time lag. These findings suggested that precipitation is a regulatory factor for TWS variations that are controlled by the amount of precipitation occurring 2 months prior in the Lancang River Basin (Fig. 12a,b). Along with climatic factors, aquifer properties, such as permeability of sediments are the main driving force behind the delayed response of TWS and precipitation. For example, in Ethiopia, a 0-month delay was recorded in karst dominated aquifers, whereas a delay of up to 6 months was observed for aquifers dominated by unconsolidated sediments (Awange et al., 2014). Similarly, the Lancang River is also dominated by karst topography with highly permeable soils; therefore, a 2-month time lag in the karst-dominated region might be a response to climate variations.

6. Conclusions

Understanding the trends in climatic variables is a practical approach for monitoring climatic changes and their impact on the hydrological cycle. A rate of decrease in precipitation of -5.03 mm/year was observed from 1998 to 2016. GLDAS and GLEAM evapotranspiration displayed an increasing trend of 4.0–4.1 mm/year from 2002 to 2020. The GRACE-TWS from JPL, GFZ, CSR-M, and JPL-M exhibited a decreasing trend from 2002 to 2016. JPL indicated a decreasing trend of -3.3 mm^{-yr}, CSR -4.0 mm/year, GFZ -3.2 mm/year, CSR-M -5.0 $mm/year^{-}$, and JPL-M -5.9 mm/year. However, the CSR-M and JPL-M solutions revealed a more severe and much wider TWS reduction in the study region than the three SH solutions. Correspondingly, GLDAS-TWS presented a decreasing trend of -4.0 mm/year, consistent with CSR, GFZ, and JPL solutions, unlike the two mascon products. The total basin discharge calculated by the water balance method showed a significant decreasing trend from 2002 to 2015. Spatial and temporal temperature trends indicated intense warming in the basin, with mean temperature increasing by 0.05 °C from 2002 to 2015. Additionally, a 2-month lag between the GRACE-derived TWS and precipitation was recorded. In addition to the aquifer properties, climatic factors could be the key drivers behind this phenomenon. However, further investigations are needed to evaluate the direct relationship involved in the

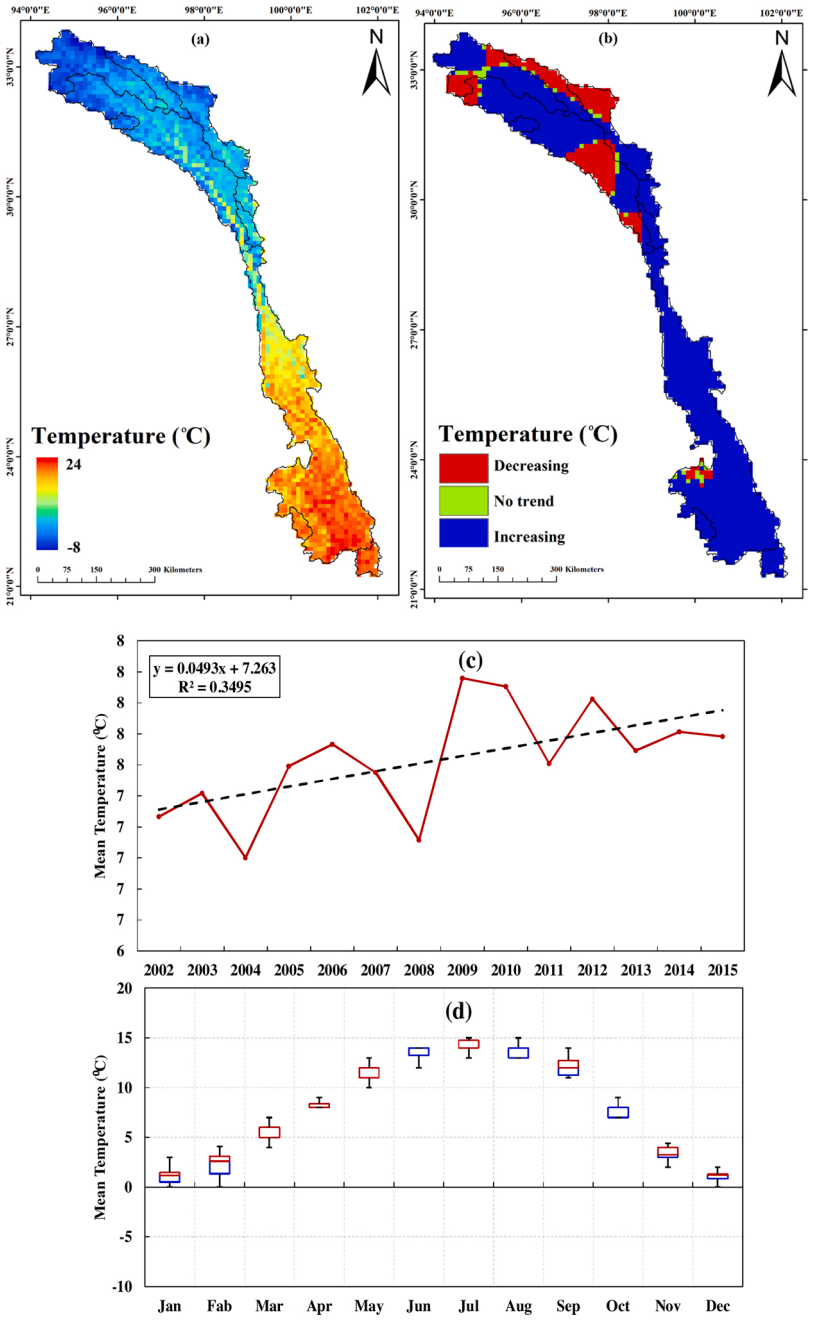

Fig. 12. Spatial distribution of temperature (a), M-K trends (b), temporal linear trend (c), and seasonality (d) across Lancang basin.

delayed response between precipitation and TWS climatology.

The present study identified multiple spatial and temporal trends for climate variables and multi-source TWS variations in the Lancang River Basin. These results could help understand climate change response in the transboundary river system and provide baseline information for water resource management for future socioeconomic development in this region.

All persons who meet authorship criteria are listed as authors, and all authors certify that they have participated sufficiently in the work to take public responsibility for the content, including participation in the concept, design, analysis, writing, or revision of the manuscript. Furthermore, each author certifies that this material or similar material has not been and will not be submitted to or published in any other publication before its appearance in the *Journal of Hydrology: Regional Studies*.

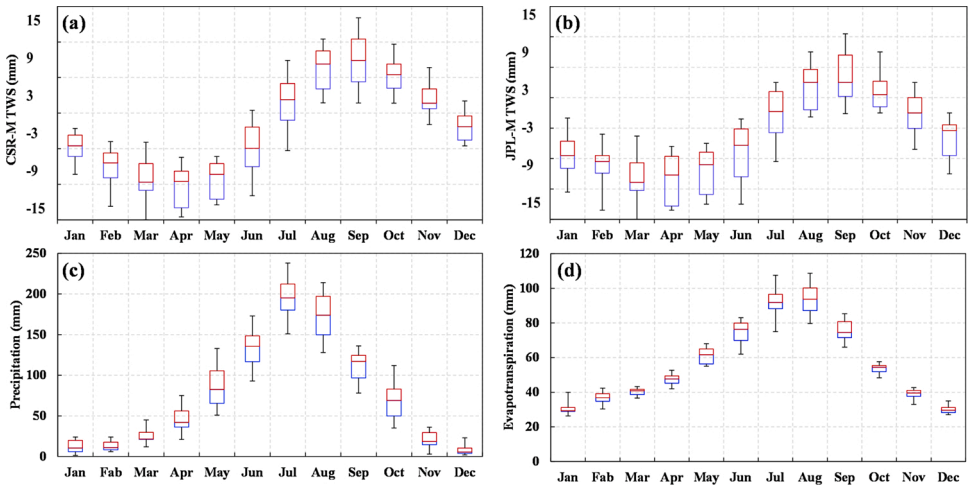

Fig. 13. Mean monthly TWS from CSR_M (a), JPL_M (b), mean precipitation (c) and evapotranspiration (d) from 2002–2016.

Declaration of Competing Interest

All authors have participated in (a) conception and design, or analysis and interpretation of the data; (b) drafting the article or revising it critically for important intellectual content; and (c) approval of the final version.

Acknowledgments

This research was funded by CAS Key Laboratory of Tropical Forest Ecology, Xishuangbanna Tropical Botanical Garden, Chinese Academy of Sciences; the National Natural Science Foundation of China (Postdoc project No: O9KF001B04, 41671209, U1602234, 31290221, 41961144017, 31770528), the National Key Research and Development Program of China (2016YFC0502105), and the CAS 135project (2017XTBG-T01, 2017XTBG-F01).

References

Andam-Akorful, S.A., Ferreira, V.G., Awange, J.L., Forootan, E., He, X.F., 2015. Multi-model and multi-sensor estimations of evapotranspiration over the Volta Basin, West Africa. Int. J. Climatol. 35, 3132–3145. https://doi.org/10.1002/joc.4198.

Andrew, R., Guan, H., Batelaan, O., 2017. Estimation of GRACE water storage components by temporal decomposition. J. Hydrol. 552.

Awange, J.L., Gebremichael, M., Forootan, E., Wakbulcho, G., Anyah, R., Ferreira, V.G., Alemayehu, T., 2014. Characterization of Ethiopian mega hydrogeological regimes using GRACE, TRMM, and GLDAS datasets. Adv. Water Resour. 74, 64–78. https://doi.org/10.1016/j.advwatres.2014.07.012.

Bibi, S., Wang, L., Xiuping, L., Jing, Z., Deliang, C., Tandong, Y., 2018. Climatic and associated cryospheric, biospheric, and hydrological changes on the Tibetan Plateau: a review. Int. J. Climatol. https://doi.org/10.1002/joc.5411.

Bibi, S., Wang, L., Xiuping, L., Xiaotao, Z., Deliang, C., 2019. Response of groundwater storage and recharge in the Qaidam Basin (Tibetan Plateau) to climate variations from 2002 to 2016. J. Geophys. Res. Atmos. https://doi.org/10.1029/2019JD030411.

Eyler, Brian, 2020. Science Shows Chinese Dams are Devastating the Mekong. Foreign Policy 22.

Ferreira, V., Gong, Z., He, X., Zhang, Y., Andam Akorful, S., 2013. Estimating total discharge in the Yangtze River Basin Using satellite-based observations. Remote Sens. 5, 3415–3430. https://doi.org/10.3390/rs5073415.

Ferreira, V.G., Yong, B., Tourian, M.J., Ndehedehe, C.E., Shen, Z., Seitz, K., Dannouf, R., 2020. Characterization of the hydro-geological regime of Yangtze River basin using remotely-sensed and modeled products. Sci. Total Environ. 718, 137354 https://doi.org/10.1016/j.scitotenv.2020.137354.

Gao, H., Tang, Q., Ferguson, C.R., Wood, E.F., Lettenmaier, D.P., 2010. Estimating the water budget of major US river basins via remote sensing. Int. J. Remote Sens. 31 (14), 3955–3978. https://doi.org/10.1080/01431161.2010.483488.

Hasson, S., Pascale, S., Lucarini, V., Böhner, J., 2016. Seasonal cycle of precipitation over major river basins in South and Southeast Asia: a review of the CMIP5 climate models data for present climate and future climate projections. Atmos. Res. 180, 42–63.

Jing, W., Yao, L., Zhao, W., Zhang, P., Liu, Y., Xia, X., Song, J., Yang, J., Li, y., Zhou, C., 2019. Understanding terrestrial water storage declining trends in the Yellow River Basin. J. Geophys. Res. Atmos. https://doi.org/10.1029/2019JD031432.

Jing, W., XZhao, X., Yao, L., Jiang, H., Xu, J., Yang, J., Li, Y., 2020. Variations in terrestrial water storage in the Lancang-Mekong river basin from GRACE solutions and land surface model. J. Hydrol. 580, 124258.

JPL, 2018. GLDAS Land Water Content Goddard Earth Sciences Data and Information Services Center. Kendall, M.G., 1955. Rank Correlation Methods, 2nd ed.

Kendall, M.G., 1975. Rank correlation methods. Griffin, London.

Landerer, W., Swenson, S., 2012b. Accuracy of scaled GRACE terrestrial water storage estimates. Water Resour. Res. 48 (4), 4531.

Li, S., He, D., 2008. Water level response to hydropower development in the upper Mekong River. AMBIO 37, 170–176.

Liu, Z., Yao, Z., Huang, H., Wu, S., Liu, G., 2014. Land-use and climate changes and their impacts on runoff in the Yarlung Zangbo River basin. China. Land Degradation & Dev. 25, 203–215.

Liu, H., Wang, Z., Ji, G., Yue, Y., 2020. Quantifying the impacts of climate change and human activities on runoff in the Lancang River Basin Based on the budyko hypothesis. Water 12, 3501. https://doi.org/10.3390/w12123501.

Long, D., Scanlon, B., Longuevergne, L., Sun, A., Fernando, D., Save, H., 2013. GRACE satellite monitoring of large depletion in water storage in response to the 2011 drought in Texas. Geophys. Res. Lett. 40 (13), 3395–3401. https://doi.org/10.1002/grl.50655.

Lv, M., Ma, Z., Yuan, X., Lv, M., Li, M., Zheng, Z., 2017. Water budget closure based on grace measurements and reconstructed evapotranspiration using GLDAS and water use data for two large densely-populated mid-latitude basins. J. Hydrol. 168, 177–193. https://doi.org/10.1016/j.jhydrol.2017.02.027.

Mann, H.B., 1945. Nonparametric tests against trend. Econometrica 13, 245–259.

Mavromatis, T., Stathis, D., 2011. Response of the Water Balance in Greece to Temperature and Precipitation Trends. Theor. Appl. Climatol. 104, 13–24. https://doi.org/10.1007/s00704-010-0320-9.
Pokhrel, Y., 2018. A review of the integrated effects of changing climate, land use, and dams on Mekong River Hydrology. Water 10 (3), 266.
Purcell, A., Tregoning, P., Dehecq, A., 2016. An assessment of theICE6G_C (VM5a) glacial isostatic adjustment model. J. Geophys. Res. Solid Earth 121 (5), 3939–3950. https://doi.org/10.1002/2015jb012742.
Qiao, L., Shiyin, L., Wanqin, G., Yong, N., Donghui, S., Junli, X., Xiaojun, Y., 2015. Glacier changes in the Lancang River Basin, China, between 1968-1975 and 2005-2010. Arctic, Arctic, Antarctic, and Alpine Res. 47, 335–344. https://doi.org/10.1657/AAAR0013-104.
Ramillien, G., Frappart, F., Guntner, A., Ngoduc, T., Cazenave, A., Laval, K., 2006. Time variations of the regional evapotranspiration rate from Gravity Recovery and Climate Experiment (GRACE) satellite gravimetry. Water Resour. Res. 42, W10403. https://doi.org/10.1029/2005WR004331.
Rodell, M., 2004. Basin scale estimates of evapotranspiration using GRACE and other observations. Geophys. Res. Lett. 31 (20) https://doi.org/10.1029/2004gl020873.
Sakumura, C., Bettadpur, S., Bruinsma, S., 2014. Ensemble prediction and intercomparison analysis of GRACE time-variable gravity field models. Geophys. Res. Lett. 41, 1389–1397. https://doi.org/10.1002/2013GL058632.
Save, H., Bettadpur, S., Tapley, B.D., 2016. High-resolution CSR GRACE RL05 mascons. Geophys. Res. Solid Earth 121 (10), 7547–7569. https://doi.org/10.1002/2016jb013007.
Scanlon, B.R., et al., 2016b. Global evaluation of new GRACE mascon products for hydrologic applications. Water Resour. Res. 52.
Scanlon, B.R., Zhang, Z., Save, H., Sun, A.Y., Müller, S.H., Van Beek, L.P.H., et al., 2018. Global models underestimate large decadal declining and rising water storage trends relative to grace satellite data. Proc. Natl. Acad. Sci. 115 (6), 1080–1089. https://doi.org/10.1073/PNAS.1704665115.
Seyoum, W., Milewski, M., 2017. Improved methods for estimating local terrestrial water dynamics from GRACE in the Northern High Plains. Adv. Water Resour. 110.
Song, Y., Fangli, Q., Zhenya, S., 2012. Improved simulation of the South Asian summer monsoon in a coupled GCM with a more realistic ocean mixed layer. J. Atmos. Sci. 1681–1690.
Syed, T.H., Famiglietti, J.S., Rodell, M., Chen, J., Wilson, C.R., 2008. Analysis of terrestrial water storage changes from GRACE and GLDAS. Water Resour. Res. 44 (2), 339–356. https://doi.org/10.1029/2006WR005779.
Tabari, H., Marofi, S., 2011. Changes of pan evaporation in the West of Iran. Water Resour. Manag. 25 (1), 97–111.
Tang, Q., 2010. Dynamics of terrestrial water storage change from satellite and surface observations and modeling. J. Hydrometeorol. 11 (1), 156–170. https://doi.org/10.1175/2009jhm1152.1.
Thompson, S.E., Harman, C.J., Troch, P.A., Brooks, P.D., Sivapalan, M., 2011. Spatial scale dependence of ecohydrologically mediated water balance partitioning: a synthesis framework for catchment ecohydrology. Water Recour. Res. 47, W00J03.
Vishwakarma, B.D., Devaraju, B., Sneeuw, N., 2018. What is the spatial resolution of GRACE satellite products for hydrology? Remote Sens. 10, 1–17. https://doi.org/10.3390/rs10060852.
Wahr, J., Swenson, S., Zlotnicki, V., Velicogna, I., 2004. Time-variable gravity from GRACE: first results. Geophys. Res. Lett. 31, L11501. https://doi.org/10.1029/2004GL019779.
Wang, P., Clemens, S., Beaufort, L., Braconnot, P., Ganssen, G., Jian, Z., Sarnthein, M., 2005. Evolution and variability of the Asian monsoon system: state of the art and outstanding issues. Quat. Sci. Rev. 24, 595–629.
Watkins, M.M., Wiese, D.N., Yuan, D.-N., Boening, C., Landerer, F.W., 2015. Improved methods for observing Earth's time variable mass distribution with GRACE using spherical cap mascons. J. Geophys. Res. Solid Earth 120 (4), 2648–2671. https://doi.org/10.1002/2014jb011547.
Xie, Z., Huete, A., Restrepo-Coupe, N., Ma, X., Devadas, R., Caprarelli, G., 2016. Spatial partitioning and temporal evolution of Australia's total water storage under extreme hydroclimatic impacts. Remote Sens. Environ. 183 (C), 43–52.
Xu, M., Kang, S., Chen, X., Wu, H., Wang, X., Su, Z., 2018. Detection of hydrological variations and their impacts on vegetation from multiple satellite observations in the Three-River Source Region of the Tibetan Plateau. Sci. Total Environ. 639, 1220–1232. https://doi.org/10.1016/j.scitotenv.2018.05.226.
Yang, C., Yu, Z., Hao, Z., Zhang, J., Zhu, J., 2012. Impact of climate change on flood and drought events in Huaihe River Basin, China. Hydrology Research 43 (1–2), 14–22.
Yang, J., Chen, H., Nie, Y., Wang, K., 2019. Dynamic variations in profile soil water on karst hill slopes in Southwest China. CATENA 172, 655–663. https://doi.org/10.1016/j.catena.2018.09.032.
Yao, T., 2012. Different glacier status with atmospheric circulations in Tibetan Plateau and surroundings. Nat. Clim. Chang. 2 (9), 663–667. https://doi.org/10.1038/nclimate1580.
Yi, S., Wang, Q., Sun, W., 2016. Basin mass dynamic changes in China from GRACE based on a multi basin inversion method. J. Geophys. Res. Solid Earth 121, 3782–3803. https://doi.org/10.1002/2015JB012608.